Tandem-Hopped OFDM Communications in Spectral Gaps of FM Noise Radar

Brandon Ravenscroft[1], Patrick M. McCormick[1], Shannon D. Blunt[1], John Jakabosky[2], and Justin G. Metcalf[3]
[1]University of Kansas – Radar Systems Lab, Lawrence, KS, USA
[2]Naval Research Laboratory – Radar Division, Washington, DC, USA
[3]Air Force Research Laboratory – Dayton, OH, USA

***Abstract* – It was recently demonstrated that hopped spectral gaps can be incorporated into a physically realizable form of FM noise radar emission. Here it is shown using experimental loopback measurements how OFDM communications can be embedded into these spectral gaps and, by virtue of proper spectral shaping, realize a composite emission with low autocorrelation sidelobes. The impact of tandem hopping of the radar spectral gap and embedded communication signal is evaluated. An example of a spectrally shaped OFDM emission for use in a notional commensal radar setting is also presented.**

I. Introduction

Many of the bands once designated for radar operation have been, and continue to be, auctioned off for commercial communications [1]. This loss combined with increasing spectral congestion [2,3] is driving research into methods for spectral cohabitation of radar and communications, either as a means to better mitigate mutual interference or to facilitate multi-function systems (e.g. [4-20]).

Here we explore one such method whereby a spectral gap within a physical radar emission is hopped in tandem with a communication signal. To facilitate this hopping behavior a nonlinear, non-recurring FM continuous wave structure denoted as pseudo-random optimized (PRO) FMCW [21,22] is employed. It was recently demonstrated experimentally [16] that hopped spectral gaps can be readily incorporated into the PRO-FMCW formulation due to its inherently changing nature (the same also holds true for the pulsed version [23]).

The communication signal being considered to occupy the hopped spectral gap is a form of orthogonal frequency division multiplexing (OFDM) [24], which is widely used in latest-generation communication systems. It is well known that OFDM signals must contend with the peak-to-average power ratio (PAPR) problem that tends to preclude operating the power amplifier in saturation, and which also limits the utility of OFDM to construct radar waveforms [25]. However, OFDM does readily permit spectral shaping, which is advantageous for this tandem-hopped formulation. Taken as a whole, this joint radar-communication emission scheme is referred to as Tandem-Hopped Radar and Communications (THoRaCs).

II. Spectrum Shaping Optimization

The PRO-FMCW emission [21] is designed on a segment-wise basis, with each segment initialized by a random FM waveform via [26] and then optimized to provide a Gaussian power spectrum. The (approximate) Gaussian power spectrum for each segment likewise realizes a Gaussian-like autocorrelation with low range sidelobes. Further, the random initialization introduces diversity among the segments such that each is unique (or at least sufficiently so for practical purposes), and thus the respective range sidelobes do not combine coherently when performing Doppler processing across the segments. As such, the non-repeating structure serves to further reduce the range sidelobes and provides a thumbtack ambiguity function in delay/Doppler.

The Gaussian power spectrum is denoted as $|G(f)|^2$, with spectral gaps introduced through the enforcement of [22]

$$|G(f)| = 0 \quad \text{for} \quad f \in \Omega, \tag{1}$$

where Ω constitutes the frequency interval(s) of the spectral gap(s). Noting that (1) realizes a rectangular shaped spectral gap, a $\sin(x)/x$ roll-off in range sidelobes arises in the autocorrelation response unless appropriate tapering of the gap is employed [16]. Here such tapering is unnecessary as the spectral gap will be filled with an OFDM signal that is spectrally shaped to blend in with the radar spectral roll-off.

Prior to optimization, the mth segment is initialized with the length T random FM signal $p_{0,m}(t)$ obtained from a random instantiation of parameters of the polyphase-code FM (PCFM) implementation [26]. From this initial random FM structure the mth optimized waveform segment is then realized by performing K iterations of the alternating projections

$$r_{k+1,m}(t) = \mathbb{F}^{-1}\left\{ |G(f)| \exp\left(j\angle \mathbb{F}\left\{ p_{k,m}(t) \right\} \right) \right\} \tag{2}$$

and

$$p_{k+1,m}(t) = u(t) \exp\left(j\angle r_{k+1,m}(t) \right), \tag{3}$$

where $u(t)$ is a length T rectangular window, $\mathbb{F}$ and $\mathbb{F}^{-1}$ are the Fourier and inverse Fourier transforms, respectively, and $\angle(\bullet)$ yields the phase of the argument.

For relatively shallow spectral gaps (~20 dB or less), defining these regions via (1) for use within (2) is sufficient. However, to obtain a greater null depth, the Reiterative Uniform Weighting Optimization (RUWO) method [27] can be employed after the K iterations of (2) and (3) as described in [22]. The final version of the mth waveform segment, obtained either with or without application of RUWO as necessary, is then phase rotated so that its initial phase value is identical the final phase value of the (m–1)th waveform segment to avoid discontinuities.

As designed here, the spectral gaps can hop at integer multiples of the waveform segment length (assuming such length is constant). Since the length of the waveform segments is arbitrary, this FMCW-based formulation can therefore realize any desired hopping rate. Also, the hopping rate need

This work was supported by a subcontract with Matrix Research, Inc. for research sponsored by AFRL under Prime Contract # FA8650-14-D-1722.

not be constant and could be changed to be shorter or longer as needed.

III. Spectral Gap Embedded Communications

Now consider the cooperative multi-function arrangement in which a communication signal is formulated to occupy simultaneously the frequency band avoided by the spectral gap in the radar emission. If the spectrum of the communications signal is shaped such that it blends well with the radar spectrum surrounding the gap, the resulting composite spectrum would appear the same as the radar emission alone, and thus provide a similar autocorrelation. A frequency-shaped OFDM signal provides a convenient way in which to achieve this attribute.

Here an OFDM implementation of a 4-QAM (π/4 phase rotation of QPSK) constellation is used for the communications signal so as to avoid the AM effects one would encounter for higher order QAM constellations. Further, because each OFDM carrier represents a narrow frequency component, shaping of the spectrum to blend in with the radar emission can be readily accomplished without altering the embedded information. For convenience we shall set the length of the OFDM symbols to be the same as the length of a radar waveform segment, though such is not necessarily required. Thus for the mth symbol interval the communication signal is

$$r_m(t) = \sum_{n=0}^{N-1} a_{m,n} \exp[\,j(2\pi f_{m,n} t + \varphi_{m,n})], \tag{4}$$

where N is the number of subcarriers, $f_{m,n}$ is the frequency of the nth subcarrier, $\varphi_{m,n}$ is the 4-QAM constellation phase value encoded onto the nth subcarrier, and $a_{m,n}$ is an amplitude scaling used to shape the spectrum for the nth subcarrier.

IV. Measured Performance Evaluation

Loopback experimental measurements of this tandem-hopped radar-embedded communication approach are used to assess performance for three different test cases. The first case considers a spectral gap and OFDM subcarriers that are stationary during the entire coherent processing interval (CPI). The second and third cases allow the gap and OFDM subcarriers to hop randomly in tandem around the band to one of either 10 or 100 different prescribed spectral locations, respectively. For all three cases, the PRO-FMCW waveform has a length of T_{w} = 200 ms consisting of $M = 10^4$ segments. Each segment possesses a 3 dB bandwidth of B = 80 MHz after optimization and a per-segment length of T = 20 μs. Each segment therefore has an approximate time-bandwidth product of $BT \cong 1600$, which yields $BT \cong 1.6 \times 10^7$ over the entire M segments. Each waveform (PRO-FMCW and OFDM) was upsampled to 8 GS/s, converted to a center frequency of 3.55 GHz and physically generated using a Tektronix AWG70002A arbitrary waveform generator. Each waveform was then I/Q sampled in a loopback configuration by a Rohde & Schwarz FSW Real-time Spectrum Analyzer (RSA) at a rate of 200 MS/s. The RSA has an analysis bandwidth of 160 MHz, producing a distinct roll-off in the captured out-of-band spectral power, as was also noted in [16].

For the first case, a single stationary spectral gap is inserted into the PRO-FMCW waveform spectrum as shown in Fig. 1 with a width of B/10. A spectrally-shaped OFDM signal is then designed to occupy this gap via determination of the $a_{m,n}$ values while the N = 162 OFDM communication symbols remain arbitrary. Because it does not have constant amplitude, this spectrally-shaped OFDM signal realizes a PAPR of 15.5 dB. The power spectrum of the composite radar/communication emission (THoRaCs) is shown in Figs. 1 and 2, with PRO-FMCW with and without a spectral gap included as a reference.

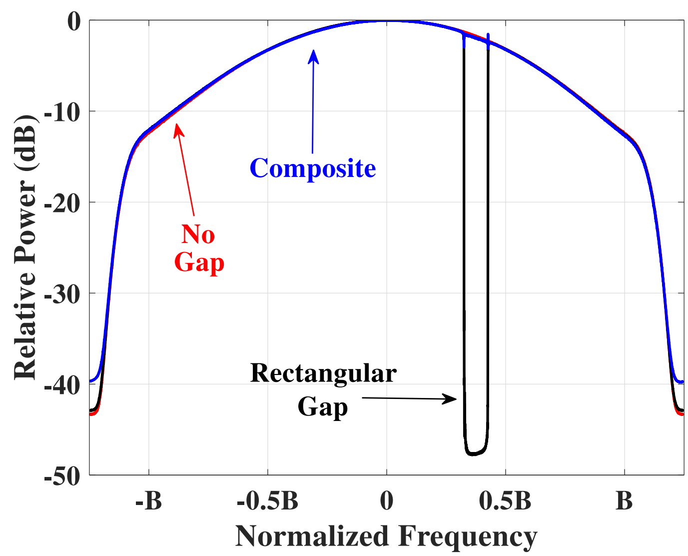

Fig. 1. Measured power spectrum of THoRaCs for fixed gap/OFDM location

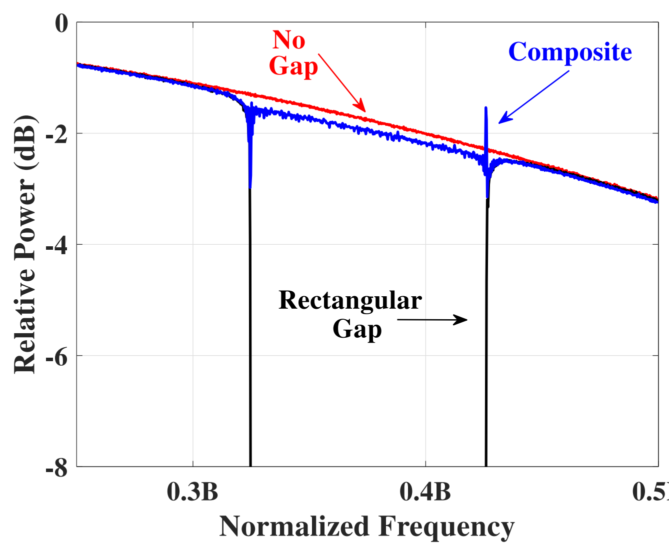

Fig. 2. Measured power spectrum of THoRaCs fixed gap/OFDM location (detail view)

The composite (blue) and rectangular gap (black) waveforms have nearly identical spectra away from the gap, which is expected since the composite waveform is formed by superimposing the gapped radar waveform with the communication signal. The composite waveform also matches well with the spectral shape of the non-gapped waveform (red) in the gap region, with the exception of the gap edges where modest deviations are observed. Here the depth of the spectral gap is about −45 dB relative to the peak, which provides more than ample signal-to-interference ratio (SIR) for the communication signal. Note that practical aspects of physical implementation (namely, power amplifier distortion) limit the achievable depth of a spectral gap, as described in [16].

Now consider the autocorrelation obtained from matched filtering the individual segments, followed by coherent integration over the M segments (i.e. Doppler processing at zero Doppler). The resulting integrated autocorrelation is depicted in Figs. 3 and 4. The non-gapped waveform (red) exhibits a peak sidelobe of −56 dB followed by very rapid sidelobe roll-off. In contrast, the rectangular gap waveform (black) has a peak sidelobe of −37 dB, with sidelobes that do not roll off into the sidelobe floor until about ±0.5T. Between these extremes, the composite waveform (blue) has a peak sidelobe of −45 dB (or −50 dB depending on how one counts the shoulder lobe) with a sidelobe roll-off that reaches the floor by ±0.3T. The composite superposition of the gapped waveform with the communications signal has thus improved the autocorrelation response compared to the gapped waveform alone. If the composite spectrum were further smoothed to eliminate the small spectral deviations observed in Fig. 2, an autocorrelation response approaching that of the non-gapped waveform would be expected.

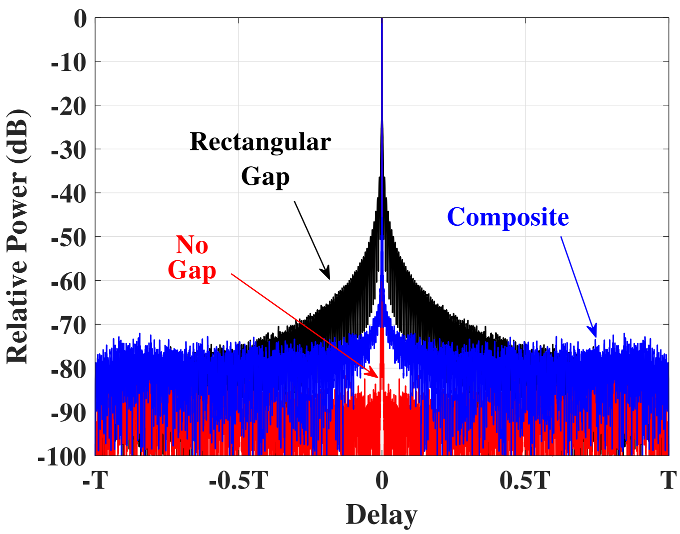

Fig. 3. Integrated autocorrelation for static gap/OFDM location

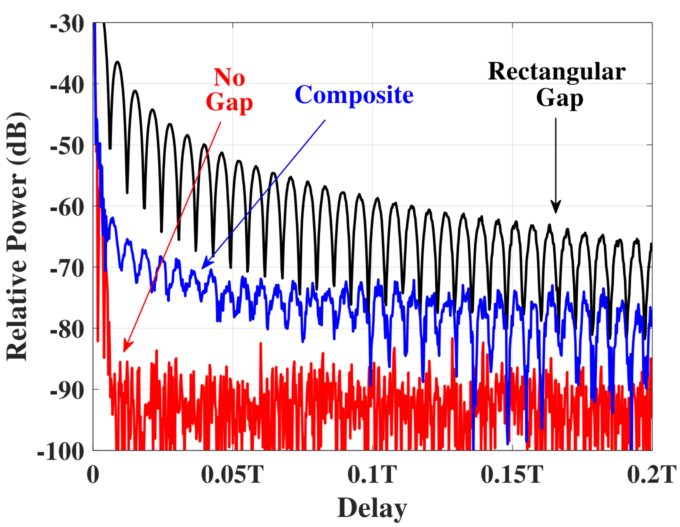

Fig. 4. Integrated autocorrelation for static gap/OFDM location (detail view)

In the second case, the total $M = 10^4$ segments are subdivided into 10 sets of 10^3 segments. For each set of segments one of the gap locations illustrated in Fig. 5 is assigned. These gap locations have $B/10$ width and do not overlap. Each location is occupied only once and the order in which they are used is randomly selected. For the total waveform duration of $T_w = 200$ ms, each gap therefore persists for $T = 20$ ms. Within each spectral gap, $N = 162$ tandem-hopped OFDM subcarriers are generated with appropriate spectral shaping to blend in with the particular gap location.

For the third case, the number of gap locations is increased to 100 while covering the same overall spectral region as the gaps in Fig. 5, with the gaps allowed to overlap. Now the M segments are subdivided into 100 sets of 10^2 segments that are randomly assigned to the 100 gap locations without repeat. In this case each tandem-hopped gap persists for $T = 2$ ms. The communication signals generated for the second and third cases have PAPR values of 15.5 dB and 15.3 dB, respectively, which is in agreement with the static gap case.

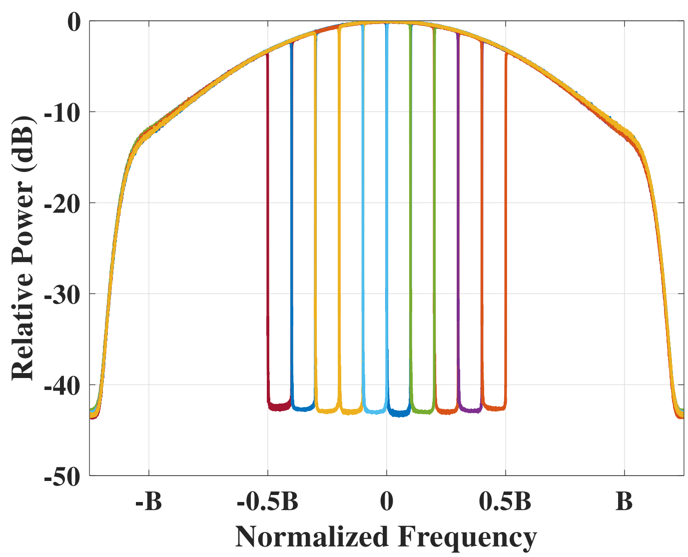

Fig. 5. Individual measured power spectrum for each randomly hopped gap

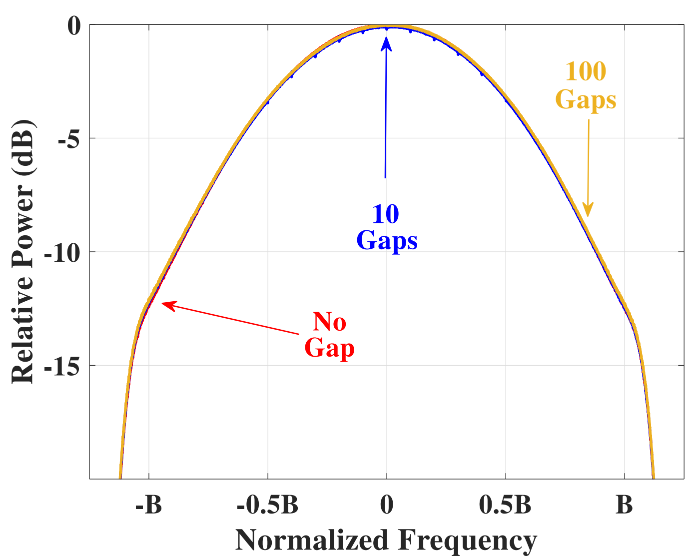

Fig. 6. Measured power spectrum for composite waveform with tandem hopping

The power spectrum of the composite emission for each of the randomly hopped cases is shown in Fig. 6. The power spectrum of a PRO-FMCW waveform with no gaps is also shown as a reference. The spectra match each other well throughout the band and the out-of-band roll-off. For the 10-gap waveform, small perturbations of the power spectrum are noted at intervals of $0.1B$, corresponding to the locations where two gaps meet. However, when the gaps are allowed to overlap, such as with the 100-gap waveform, these perturbations are smoothed out, thereby matching closely with the power spectrum of the non-gapped waveform.

Figures 7 and 8 show the integrated autocorrelation of the composite waveforms with 10 and 100 hopped gaps. The autocorrelation of a non-gapped waveform is shown for reference. All three waveforms exhibit a peak sidelobe of -56 dB at a delay of $\pm 0.0028T$. The 10-gap case contains higher sidelobes near the main lobe with a second peak of -63 dB located at $\pm 0.0065T$. Successive sidelobes appear at integer multiples of this delay until decaying into the sidelobe floor. This sidelobe effect is an artifact of the non-overlapping gap location structure used to form the spectrum.

The autocorrelation for the 100-gap case matches much closer to that of the non-gapped case, having a -70 dB sidelobe level at the second peak near the main lobe. The next peak sidelobe level for this case is -76 dB and occurs at a delay of $\pm 0.065T$, a factor of 10 greater in delay than the 10 gap case, which is commensurate with the tenfold increase in gap locations. Successive sidelobe peaks occur at integer multiples in delay.

Filling the radar spectral gap with an appropriately shaped communication signal has created a composite autocorrelation response very close to that of a radar waveform with no spectral gaps. Further increasing the overlap (number of gap locations) in the randomly hopping gap structure is expected to push out the peak sidelobe locations further in delay (and with lower values) thereby producing a mean autocorrelation response nearly identical to that of a non-gapped waveform. Perturbing the gap locations may also break up the structure to further reduce these sidelobes.

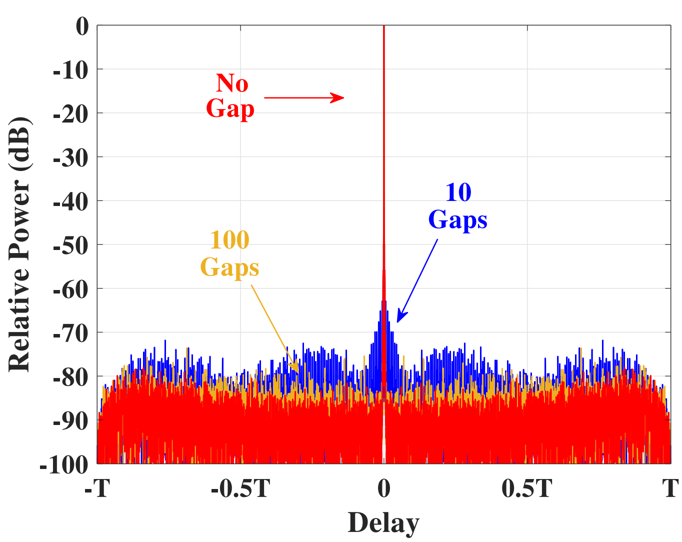

Fig. 7. Integrated autocorrelation with a randomized tandem hopping

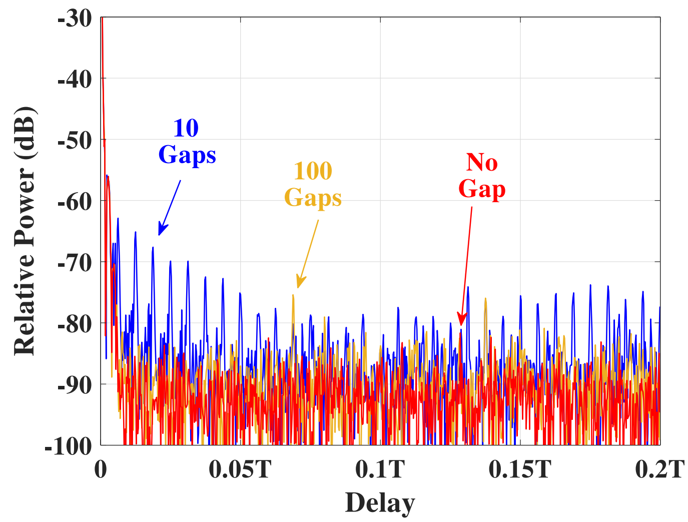

Fig. 8. Integrated autocorrelation with randomized tandem hopping (detail view)

The autocorrelation plots shown in Figs. 3, 4, 7 and 8 illustrate the response to a stationary point target. However, hopping of a spectral gap during the CPI was shown to degrade Doppler processing in [16]. To assess how filling the spectral gap with OFDM subcarriers has improved the Doppler response, the range-Doppler point spread function is generated for the composite waveform in the tandem hopped cases (10 and 100 gap locations). The segments of each waveform are pulse compressed and Doppler processed by weighting the segments with a Taylor window and then performing a Fourier transform across the 10^4 segments in each 200 ms waveform. A center frequency of 3.55 GHz and a post-optimization bandwidth of 80 MHz are still employed.

Figures 9 and 10 show close-up regions of the range-Doppler point spread function for the 10 and 100 gap randomized tandem hopped cases, respectively. Both composite waveforms have energy spread in range and Doppler that is not suppressed by the Taylor window. The energy spread is more severe for the 100 hopped gap case, which is expected since the hopping rate has increased. However, the energy spread in both cases is much less than that observed in [16] for an unfilled, randomly hopped and tapered gap allowed to occupy 10 random spectral locations during the CPI. Thus, in addition to facilitating a multi-function radar/communication capability, filling the randomly hopped spectral gap with spectrally-shaped OFDM subcarriers has improved the range-Doppler response relative to the case where the gap is not filled.

V. Commensal Radar

Finally, given that the spectrally-shaped OFDM signal can be used both as a communication signal and to mimic a useful component of the radar spectrum within the composite waveform above, it is logical to also consider the extreme case of constructing the entire radar signal from spectrally-shaped OFDM. Because the communication symbols remain completely arbitrary (it is the Gaussian-like power spectrum that provides good autocorrelation) such an emission could in principle be used to leverage a primary communication emission having this structure to perform passive radar as well

[28-30]. Griffiths, Darwazeh, and Inggs recently proposed this general manner of operation as “commensal radar” [31], in which the communication emission is designed to also serve the secondary purpose of being a useful illumination for passive radar.

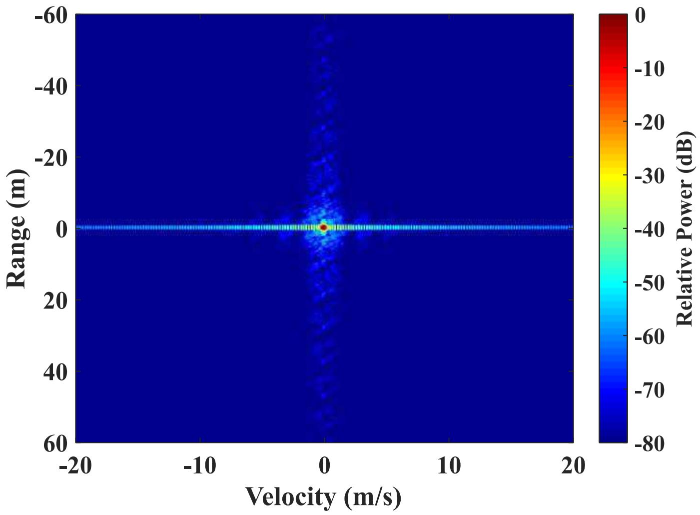

Fig. 9. Range-Doppler point spread function with 10 randomly hopped gap locations

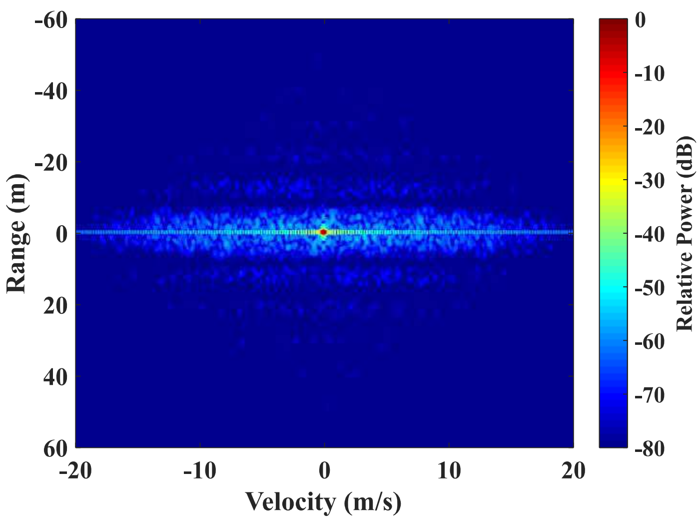

Fig. 10. Range-Doppler point spread function with 100 randomly hopped gap locations

To illustrate this case, Fig. 11 shows the experimentally measured power spectrum of a commensal emission based on the spectrally-shaped OFDM structure of (4) where $N = 3000$ subcarrier frequencies now occupy the entire band and are shaped to provide a Gaussian power spectrum (the Gaussian spectral template is included as a reference). Deviations at the band edges are again a by-product of the analysis bandwidth limitation of the RSA.

As with the other spectrally-shaped non-repeating waveforms, the OFDM emission exhibits a thumbtack delay/Doppler ambiguity function (not shown). The integrated autocorrelation response for this case is depicted in Figs. 12 and 13. Compared to the non-gapped PRO-FMCW waveform, the sidelobe floor is ~10 dB higher, though still low with a –56 dB peak, thus matching that of the non-gapped waveform.

Like all OFDM signals, the PAPR may be high (here it is 15.5 dB). The impact of pilot symbol ambiguities [30] is also not included here, though a randomization of such should also prove useful for a secondary passive radar application. Finally, a Gaussian spectral shape would also clearly deviate from one that maximizes information capacity. However, an analysis of the performance trade-off between capacity and ambiguity function utility may well yield power spectral shapes that adequately balance between the communication and radar modes for this manner of operation.

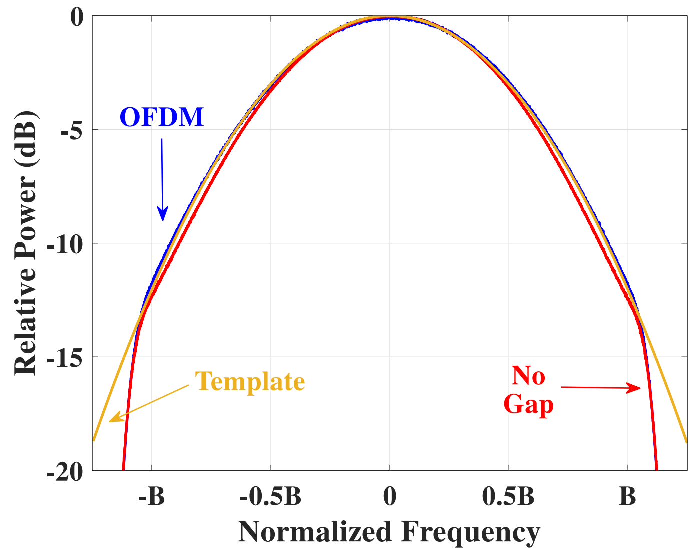

Fig. 11. Measured power spectrum of spectrally-shaped OFDM used as a commensal waveform

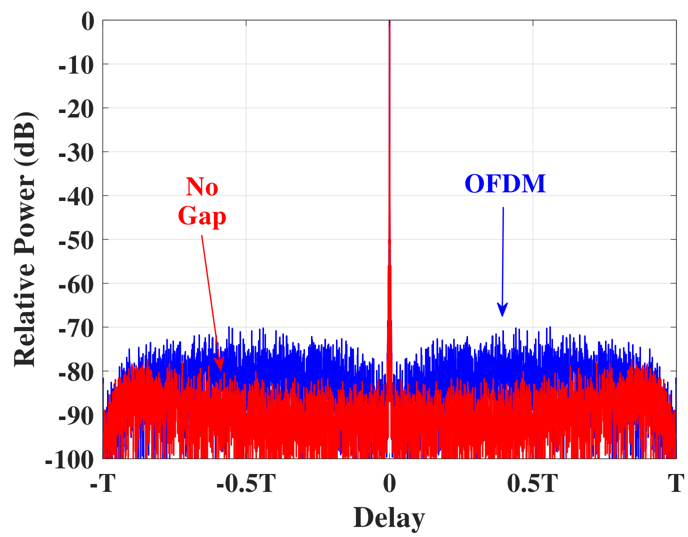

Fig. 12. Integrated autocorrelation of spectrally-shaped OFDM used as a commensal waveform

VI. Conclusions

Filling spectral gaps in the PRO-FMCW waveform with shaped OFDM subcarriers has been experimentally shown to create a more favorable autocorrelation response (when using the composite emission to match filter) than a waveform where the spectral gap is not filled. It was demonstrated that the gap and OFDM carriers can be hopped in tandem inside the spectral band at different rates and that allowing the gap locations to overlap improves the mean autocorrelation response of the composite waveform. A "commensal radar" waveform was also shown to provide good autocorrelation characteristics while serving a primary communication function.

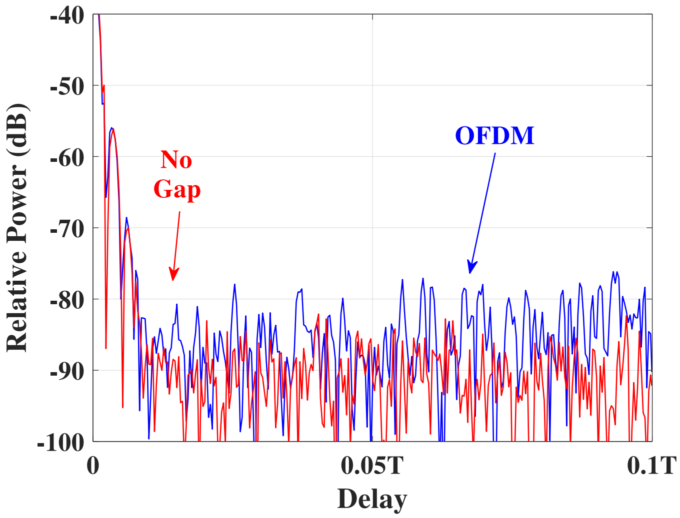

Fig. 13. Integrated autocorrelation of spectrally-shaped OFDM used as a commensal waveform (detail view)

REFERENCES

[1] Federal Communcations Commission, "National broadband plan," Available: http://www.broadband/gov.

[2] H. Griffiths, L. Cohen, S. Watts, E. Mokole, C. Baker, M. Wicks, S. Blunt, "Radar spectrum engineering and management: technical and regulatory Issues," *Proc. IEEE*, vol. 103, no. 1, pp. 85-102, Jan. 2015.

[3] H. Griffiths, S. Blunt, L. Cohen, L. Savy, "Challenge problems in spectrum engineering and waveform diversity," *IEEE Radar Conf.*, Ottawa, Canada, Apr./May 2013.

[4] S.D. Blunt, P. Yatham, J. Stiles, "Intra-pulse radar-embedded communications," *IEEE Trans. Aerospace & Electronic Systems*, vol. 46, no. 3, pp. 1185-1200, July 2010.

[5] S.D. Blunt, M.R. Cook, J. Stiles, "Embedding information into radar emissions via waveform implementation," *Intl. Waveform Diversity & Design Conf.*, Niagra Falls, Canada, pp. 195-199, 8-13 Aug. 2010.

[6] C. Sturm, W. Wiesbeck, "Waveform design and signal processing aspects for fusion of wireless communications and radar sensing," *Proc. IEEE*, vol. 99, no. 7, pp. 1236-1259, July 2011.

[7] S.D. Blunt, J.G. Metcalf, C.R. Biggs, E. Perrins, "Performance characteristics and metrics for intra-pulse radar-embedded communications," *IEEE Journal on Selected Areas in Communications*, vol. 29, no. 10, pp. 2057-2066, Dec. 2011.

[8] A. Hassanien, M.G. Amin, Y.D. Zhang, F. Ahmad, "A dual function radar-communications system using sidelobe control and waveform diversity," *IEEE Intl. Radar Conf.*, Washington, DC, May 2015.

[9] J.G. Metcalf, C. Sahin, S.D. Blunt, M. Rangaswamy, "Analysis of symbol design strategies for intrapulse radar-embedded communications," *IEEE Trans. Aerospace & Electronic Systems*, vol. 51, no. 4, pp. 2914-2931, Oct. 2015.

[10] D. Ciunonzo, A. De Maio, G. Foglia, M. Piezzo, "Intrapulse radar-embedded communications via multiobjective optimization," *IEEE Trans. Aerospace & Electronic Systems*, vol. 51, no. 4, pp. 2960-2974, Oct. 2015.

[11] A. de Oliveira, R. Sampaio-Neto, J.M. Fortes, "Robust radar-embedded sidelobe level modulation using constrained optimization design," *IEEE Radar Conf.*, Philadelphia, PA, May 2016.

[12] B. Paul, A.R. Chiriyath, D.W. Bliss, "Joint communications and radar performance bounds under continuous waveform optimization: the waveform awakens," *IEEE Radar Conf.*, Philadelphia, PA, May 2016.

[13] J.T. Reed, J.L. Odom, R.T. Causey, A.D. Lanterman, "Gaussian multiple access channels for radar and communications spectrum sharing," *IEEE Radar Conf.*, Philadelphia, PA, May 2016.

[14] M. Scharrenbroich, M. Zatman, "Joint radar-communications resource management," *IEEE Radar Conf.*, Philadelphia, PA, May 2016.

[15] B. Li, A. Petropulu, "MIMO radar and communication spectrum sharing with clutter mitigation," *IEEE Radar Conf.*, Philadelphia, PA, May 2016.

[16] J. Jakabosky, B. Ravenscroft, S.D. Blunt, A. Martone, "Gapped spectrum shaping for tandem-hopped radar/communications & cognitive sensing," *IEEE Radar Conf.*, Philadelphia, PA, May 2016.

[17] F. Hessar, S. Roy, "Spectrum sharing between a surveillance radar and secondary wi-fi networks," *IEEE Trans. Aerospace & Electronic Systems*, vol. 52, no. 3, pp. 1434-1448, June 2016.

[18] C. Sahin, J. Jakabosky, P.M. McCormick, J.G. Metcalf, S.D. Blunt, "A novel approach to embed communication symbols into physical radar waveforms," *IEEE Radar Conf.*, Seattle, WA, May 2017.

[19] P.M. McCormick, S.D. Blunt, J.G. Metcalf, "Simultaneous radar and communication emissions from a common aperature, part I: theory," *IEEE Radar Conf.*, Seattle, WA, May 2017.

[20] P.M. McCormick, A.J. Duly, B. Ravenscroft, J.G. Metcalf, S.D. Blunt, "Simultaneous radar and communication emissions from a common aperature, part II: experimentation," *IEEE Radar Conf.*, Seattle, WA, May 2017.

[21] J. Jakabosky, S.D. Blunt, B. Himed, "Waveform design and receive processing for nonrecurrent nonlinear FMCW radar," *IEEE Intl. Radar Conf.*, Washington, DC, May 2015.

[22] J. Jakabosky, S.D. Blunt, A. Martone, "Incorporating hopped spectral gaps into nonrecurrent nonlinear FMCW radar emission," *IEEE Intl. Workshop on Computational Advances in Multi-Sensor Adaptive Processing*, Cancun, Mexico, Dec. 2015.

[23] J. Jakabosky, S.D. Blunt, B. Himed, "Spectral-shape optimized FM noise radar for pulse agility," *IEEE Radar Conf.*, Philadelphia, PA, May 2016.

[24] A.R.S. Bahai, B.R. Saltzberg, M. Ergen, *Multi-Carrier Digital Communications: Theory and Applications of OFDM*, Springer, 2004.

[25] J. Jakabosky, L. Ryan, S.D. Blunt, "Transmitter-in-the-loop optimization of distorted OFDM radar emissions," *IEEE Radar Conf.*, Ottawa, Canada, Apr./May 2013.

[26] S.D. Blunt, M. Cook, J. Jakabosky, J. de Graaf, E. Perrins, "Polyphase-coded FM (PCFM) radar waveforms, part I: implementation," *IEEE Trans. Aerospace & Electronic Systems*, vol. 50, no. 3, pp. 2218-2229, July 2014.

[27] T. Higgins, T. Webster, A.K. Shackelford, "Mitigating interference via spatial and spectral nulling," *Radar, Sonar & Navigation, IET*, vol.8, no.2, pp.84,93, Feb. 2014.

[28] D. Poullin, "Passive detection using digital broadcasters (DAB,DVB) with COFDM modulation," *IEE Radar, Sonar & Navigation*, vol. 152, no. 3, pp. 143-152, June 2005.

[29] C.R. Berger, B. Demissie, J. Heckenbach, P. Willett, S. Zhou, "Signal processing for passive radar using OFDM waveforms," *IEEE J. Selected Topics Signal Processing*, vol. 4, no. 1, pp. 226-238, Feb. 2010.

[30] J.E. Palmer, H.A. Harms, S.J. Searle, L.M. Davis, "DVB-T passive radar signal processing," *IEEE Trans. Signal Processing*, vol. 61, no. 8, pp. 2116-2126, Apr. 2013.

[31] H. Griffiths, I. Darwazeh, M. Inggs, "Waveform design for commensal radar," *IEEE Intl. Radar Conf.*, Washington, DC, May 2015.